IEEE Access
Multidisciplinary ⋮ Rapid Review ⋮ Open Access Journal

Received 20 September 2023, accepted 18 October 2023, date of publication 23 October 2023, date of current version 6 November 2023.

Digital Object Identifier 10.1109/ACCESS.2023.3327222

RESEARCH ARTICLE

Operation-Aware System Design for Synergistic Integration of Regenerative Braking Energy of Railway Systems into EV Fast Charging Stations

SEPEHR NAJAFI LARIJANI[1], SEYED SAEED FAZEL[1], MOKHTAR BOZORG[2], (Member, IEEE), AND HAMED JAFARI KALEYBAR[3], (Member, IEEE)

[1]School of Railway Engineering, Iran University of Science and Technology, Tehran 1684613114, Iran
[2]School of Management and Engineering Vaud (HEIG-VD), HES-SO University of Applied Sciences of Western Switzerland, 1401 Yverdon-Les-Bains, Switzerland
[3]Department of Energy, Politecnico di Milano, 20156 Milan, Italy

Corresponding author: Hamed Jafari Kaleybar (hamed.jafari@polimi.it)

ABSTRACT Fast charging stations (FCSs) for electric vehicles are associated with large power demands, often coinciding with peak power demands from other consumers. This places significant strain on distribution networks (DNs). To address this issue, this paper proposes a promising method that harnesses the untapped potential of electric railway systems (ERSs) and wasted regenerative braking energy (RBE) of trains in combination with a battery energy storage system (BESS) to supply EV charging station and participate in the FCS energy supply chain (FCS-ESCH). The proposed integrated approach, as the intermodal sustainable electric transportation system (SETS), aims to reduce the peak power demand of FCSs especially at strategic locations, such as parking areas close to electric railway stations and park-and-ride areas. To achieve this goal, an operation-aware optimization model is developed that determines the optimal sizes of the interfacing converter and the BESS, while also proceeding with optimal energy exchange planning. A generic model for trains' RBE production is proposed, as well, and adapted to the operation-aware optimization model to verify the effectiveness of the proposed approach by conducting simulations of a real case study that accurately replicates system behavior with the desired level of precision. Furthermore, sensitivity analyses are performed to explore the impact of varying the power rating of the interfacing converter responsible for transmitting RBE to the FCS-ESCH, as well as the per-unit price of BESS energy capacity. The results showcase the potential of employing SETS as an efficient means to mitigate the challenges associated with FCSs, especially peak shaving and cost reductions, paving the way for a more sustainable electric transportation system.

INDEX TERMS Electric railway system, fast-charging station, optimal planning, optimal sizing, regenerative braking energy.

NOMENCLATURE

INDICES

i	Index for a time step of ERS simulation.
n	Index for the train number.
v	Index for the train velocity.
x	Index for the train position.
t	Index for a time step of the LP problem.
T	Index for the final time step.
d	Index for days.
wd	Index for weekdays.
we	Index for weekends.
w	Index for weeks.
s	Index for seasons.
y	Index for years.

SIMULATION VARIABLES

$F_{i,n,x}$	The driving/deterring force of the train [kN].

The associate editor coordinating the review of this manuscript and approving it for publication was Shaohua Wan.

$F^{tr}_{i,n,x}$	Total resistive force against the train [kN].
$a_{i,n,x}$	The acceleration of the train [m/s^2].
$V_{i,n,x}$	The velocity of the train [m/s].
$V_{2_{i,n,x}}$	The velocity of the train at the updated position [m/s].
$V_{1_{i,n,x}}$	The velocity of the train at the present position at present time step [m/s].
$F^{drag}_{i,n,x}$	Aerodynamic resistive force [kN].
$F^{grad}_{i,n,x}$	Gradient resistive force [kN].
$F^{p}_{i,n,x}$	Curvature resistive force [kN].
$P^{RBE}_{d,t}$	The available RBE [kW].
$\Delta x_{i,n,x}$	The distance a train passes via specific acceleration [km].

OPTIMIZATION VARIABLES

$P^{G}_{s,d,t}$	Power flow from the DN to FCS [kW].
$P^{R}_{s,d,t}$	Power flow from the ERS to the FCS [kW].
P^{R}_{max}	Power rating of RBE converter (maximum power flow from the ERS to the FCS) [kW].
$P^{RBE}_{d,t}$	The available RBE [kW].
$SOC_{s,d,t}$	BESS state of charge [kWh].
P_{ESS}	BESS power rating [kW].
$P^{ch}_{s,d,t}$	BESS charging power [kW].
$P^{dch}_{s,d,t}$	BESS discharging power [kW].
E_{ESS}	The BESS energy capacity [kWh].
C_{OG}	The cost of electricity purchased by FCS from DN [$].
C_{OS}	The operation/maintenance cost of the BESS [$].
C_{IR}	The investment cost of the RBE converter [$].
C_{IS}	The investment cost of the BESS [$].

PARAMETERS

F^{v}_{b}	The braking force of the train's motors [kN].
TE^{v}	The tractive force of the train's motors [kN].
$M_{i,n}$	Mass of a train [tons].
$M^{eff}_{i,n}$	The effective mass of a train [tons].
st	The set of positions in the vicinity of the sample station.
μ_{curve}	The coefficient of curvature resistive force for a train.
ax	The number of the trains' axles.
ca	The number of cars per train.
ar	The frontal area of the train [m^2].
$S_{i,n}$	Gradient percent of the ERS path.
R	Rotating mass factor for the trains.
$r_{i,n}$	Curve radius of the ERS path [m].
P^{G}_{max}	Maximum power flow from the DN to FCS [kW].
$P^{L}_{d,t}$	The power demand of the FCS [kW].
η	The RBE chain efficiency.
η_{Motor}	The trains' motor efficiency.
η_{Drive}	The trains' motor drive efficiency.
η_{ch}	The BESS charging efficiency.
η_{dch}	The BESS discharging efficiency.
η_{G}	The efficiency of the DN converter.
η_{ESS}	The efficiency of the BESS converter.
η_{R}	The efficiency of the RBE converter.
Δt	The time operator for translating power to energy.
σ	The BESS leakage rate.
DoD_{min}	The BESS minimum depth of discharge.
DoD_{max}	The BESS maximum depth of discharge.
SOC^{in}_{s}	The BESS initial state of charge [kWh].
$\pi^{G}_{s,d,t}$	Price of the electricity purchased from DN [$/kWh].
π_{Rconv}	Per-unit price of the RBE Converter [$/kW].
π^{OM}_{ESS}	BESS operation/maintenance per-unit cost [$/kWyear].
π^{P}_{ESS}	The power-related per-unit price of the BESS [$/kW].
π^{E}_{ESS}	The energy-related per-unit price of the BESS [$/kWh].
q^{w}_{s}	The number of weeks in each season.
Y	The lifetime duration of the study [years].
DR	The discount rate.

I. INTRODUCTION

The growing and everlasting demand for energy and its environmental repercussions have turned into a widespread concern throughout the world. In this regard, studying transportation as a prominent sector of energy consumption and air pollution is a necessary step toward urban sustainability [1]. Since the energy consumption of electric transportation is recognized more suitable in terms of environmental issues than other conventional transportation modes, it is the most applicable. However, electrified systems cannot be merely assumed as a sustainable infrastructure for transportation unless a systematic approach is applied [2].

One of the severe challenges facing electric transportation's sustainable development is related to electric vehicles (EVs) charging infrastructures. Fast-charging stations (FCSs), with high-rated power and voltage, have drawn the most attention among the chargers, recently. An outstanding characteristic of them is their short-time charging duration [3]. Besides, the penetration of FCSs into the market is much easier than other types. Furthermore, lower operation cost and higher efficiency while keeping the average state of charge (SOC) of the batteries (for vehicle speed) are their other distinguishing features [4]. As to practicalities, fast chargers like ABB Terra 53, Tritium Veefil-RT, Tesla Supercharger, EVTEC espresso & charge, and ABB Terra HP with rated power ranging from 50 kW to 350 kW are commercially available [5].

Although the FCSs are functionally and technically beneficial, they bring about some problems that provoke the interest to conduct this study to overcome the hurdle of using FCSs.

TABLE 1. Comparison between this study and the existing literature on the integration of RBE and EV charging systems.

Case studies	Suggestion	Architectures Challenges	Real Project Report	Mathematical framework	Line loss minimization	BESS sizing	Interfacing converter of RBE sizing	RBE model	Decreasing the price of BESS	Energy exchanges planning
[22]	✓	×	×	×	×	×	×	×	×	×
[1]	×	✓	×	×	×	×	×	×	×	×
[28]	×	×	✓	×	×	×	×	×	×	×
[29]	×	×	✓	×	×	×	×	×	×	×
[30]	×	×	×	✓	×	×	×	×	×	×
[31]	×	×	×	×	✓	×	×	×	×	×
[32]	✓	×	×	×	×	×	×	×	×	×
This study	✓	✓	×	✓	×	✓	✓	✓	✓	✓

Firstly, not only does the FCSs supplying procedure stress the distribution network (DN) because of the substantial required power [6], but also their huge power demand on the DN has time overlap with other consumers' power demand. Secondly, since their development has some infrastructural setbacks like huge capital cost [7], and limited choices of feasible locations for establishment [8], [9], the inevitable increasing penetration of EVs [3] is likely to exacerbate the situation since the power demand is going to be more than the DN's bearing limits.

Therefore, the objective of this study is to resolve the difficulties of using FCSs, including their great power demand and limited potential infrastructure. In the initial phase, the pressing issue of the substantial power demand observed in FCSs during peak periods has prompted research exploration within the realm of urban sustainability and smart cities [10]. Notably, there is a growing interest in investigating the integration of various transportation modes as potential solutions. Within this context, the Electric Railway System (ERS) emerges as a particularly pertinent mode of electric transportation, characterized by its significant power interchange with the electricity network. A distinctive feature of ERS is the presence of dedicated traction power substations (TPS) [11] and their installations, which are often equipped with higher extra capacity and extensive infrastructure to manage the dynamic and fluctuating power demands [12]. Furthermore, the points of common coupling for these TPSs are frequently connected to high-voltage transmission networks [13]. Consequently, the DN experiences a more substantial load impact from FCSs compared to the ERS. Therefore, leveraging the advantages of ERS to mitigate the strain on the DN imposed by FCSs is a strategically sensible approach. This could involve harnessing the untapped potential of regenerative braking energy (RBE) produced by trains, which traditionally dissipates as heat in conventional systems. Redirecting this RBE into the FCS could contribute to a more balanced energy distribution.

Moreover, to settle the issue of limited spatial degree of freedom for the placement of FCSs, still, the synergy between the ERS and the FCS could be a neat solution since ERS could share its spaces so that the FCS could exploit the ERS's infrastructure as a step to fulfill the potential of increasing EVs' emergence. Accordingly, this study aims to explore the integration of two crucial electric transportation modes. This pursuit seeks to establish a Sustainable Electric Transportation System (SETS) that effectively tackles the challenges posed by FCSs. The proposed framework envisions collaborative use of RBE and Battery Energy Storage Systems (BESS), leveraging the intermittent nature of RBE. This strategy has the potential to strengthen the FCS energy supply chain (FCS-ESCH) and enhance the overall efficiency of the transportation system.

A. LITERATURE REVIEW

The literature review initiates with two essential pillars, and then it follows with the main idea of this study. The two initiatives are the surveys on 1) The taken steps to mitigate the negative effects of FCSs. 2) Applications of trains' RBE. Which results in a state-of-the-art idea: 3) The contribution of trains' RBE to FCS-ESCH.

To overcome the hurdles related to FCSs, the utilization of an energy storage system (ESS) has been investigated in some studies like [14], where the reduced value of power demand has been achieved in [15], although the optimal sizing of which has not been taken into account. Subsequently, ESS's sizing is taken into account in another research [3]. Moreover, researchers surveyed the photovoltaic (PV) energy as a distributed generation (DG) in FCS supplying architecture [6] that shows the profitability of mixing ESS and PV panels. Likewise, this scenario is considered in [16] when rule-based energy management has been defined. However, simultaneous optimal sizing of the PV panel and the ESS seems to be crucial in the economic viability of the FCS, since investment costs of PV panels incur high costs to the FCS's owner; thus a feasibility study is needed which is taken into account in [17]. With respect to taking a step to address the infrastructural challenges like the lack of feasible locations for constructing charging stations, mobile chargers are taken into consideration in [18] to provide better availability, where companies like EVESCO [19] and Volkswagen [20] have offered mobile fast chargers to market. Nonetheless, such a solution has the downside of production cost which should be investigated to see if it is feasible or not.

On the other hand, RBE in the ERS is a unique energy source that is likely to play a similar role as DGs. RBE is the electrical energy that could be recovered instead of being wasted as heat during the trains' braking procedure. Some research (e.g. [21]) investigates three main perspectives on applications of RBE recovery, i.e. time scheduling for supplying other trains, exploiting ESSs for saving energy, and bilateral ERS substations that are elaborated as follows. Time management for reusing the trains' RBE in close accelerating trains is not necessarily applicable because of the incompatibility of acceleration and braking times through the ERS [22], and the attempts to adapt them to happen simultaneously may result in operational restrictions. Subsequently, ESSs could substantially contribute to serving the purpose of recovering energy [23], although their usage may impose energy losses and costs. Lastly, the bilateral substations concept contends that selling back the energy to the main grid seems affordable when the electricity market buys the energy at an interesting price [24]. Later, using the regenerated energy for auxiliary loads has been proposed in [25], when energy loss during the DC to AC conversion is a serious hindrance. Besides, the idea of reusing the energy for the train's auxiliary load is in vain since the amount of its demand is very low [26]. Subsequently, in [27], the author has considered the battery of EVs as an ESS to exchange the energy through the ERS, which is seen to be an extravagance with converting and charging/discharging procedure, when the energy could be used by the EVs themselves. However, there is an apparent lack of research on RBE usage in EV-charging infrastructures, and the limited studies in this regard are surveyed as follows.

Reference [22] stated that a service provider, selling the energy to the FCS, could be a medium voltage distribution system operator or an external company like ERS. The proposal suggests using ERS to supply FCS-ESCH with trains' RBE, leveraging its network advantage. However, no prior investigation or mathematical model exists for this integration.

In [1], ERS is proposed as a smart microgrid that tends to manage the power flow collection and consequently delivers it to EV charging stations in the form of an energy hub without a modeled framework for a feasibility study. It just discussed the possible architectures, challenges, advantages, and obstacles related to the integration of DGs, ESSs, and EV-charging infrastructures. In [32] also a bilateral system has been proposed. In that system, EVs can supply accelerating trains or consume trains' RBE. Nonetheless, the feasibility study of such a system has not been presented in the form of a mathematical framework. Moreover, in [28], ERS-FCS integration's functionality in the ELIPTIC project is just pointed out where the FCS for individual vehicles and public electric buses is considered. Another study related to the Train2Car project in Madrid defines different energy management strategies for integrating ERS and ESS into the FCS-ESCH to control the power flow; however, the ESS sizing and operation planning are not implemented studied [29]. In a piece of recent research [30], such a configuration has been propounded in which an energy management system was taken into consideration. Nonetheless, this research has neglected to provide a model for RBE. This research also overlooks the cost of the RBE converter which prevents us from using unlimited RBE generations and neither BESS nor any of the converters in the configuration have been sized. Ultimately, in [31], the authors just tried to minimize the total line loss in a configuration in which RBE was considered to be utilized in EV charging systems. Therefore, despite the clear motivation for ERS-FCS integration, a comprehensive feasibility study that considers the necessary constraints in a rigorous mathematical framework has not been done in the literature as shown in Table 1. This is why this study's contribution is as follows.

B. CONTRIBUTION

This study innovatively addresses gaps in the literature regarding FCS for EVs, railway network integration, and train-to-vehicle concepts. The previous studies have not fully harnessed the potential of trains' RBE. Moreover, all the few articles published dealing with the integration of ERS into the EV charging system discussed energy transfer and optimization, without any specific attention to the sizing of existing interface converters. Accordingly, the main contributions of this study can be summarized as follows:

- Introduction of indirect train-to-vehicle technology in park-and-ride areas, utilizing train RBE to charge EVs.
- Development of an operation-aware optimization model for determining optimal converter size and BESS capacity, proceeding with efficient energy exchange planning.
- Introduction of a tailored model for RBE generation, offering a more accurate representation within the context of FCS for EVs.
- Application of the approach to a real-world case study, providing practical insights into the feasibility and benefits of implementing SETS.
- Conducted sensitivity analyses, enriching findings, and offering nuanced insights into system performance under various configurations.
- Holistic mitigation of adverse impacts by establishing a clear link between the harnessed RBE and BESS integration.

C. PAPER ORGANIZATION

The rest of the paper is organized as follows: Section II describes the proposed SETS configuration, its technical concerns, and subsequently, its operation-aware optimization model is introduced. In Section III, the linear programming (LP) problem of the operation-aware optimization model is formulated and explained. Section IV presents the ERS modeling and simulation process to achieve the RBE model. In section V, numerical results are presented and parameter impacts, energy exchanges, purchased electricity from DN,

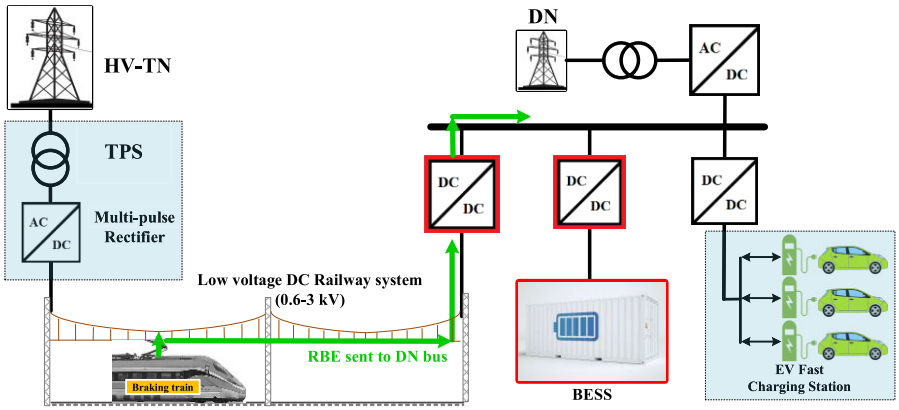

FIGURE 1. Proposed SETS configuration for utilizing RBE of trains.

and sensitivity analyses are discussed to explore the feasibility and effectiveness of employing SETS for a real case study. Finally, the conclusions are presented in Section VI.

II. PROPOSED SETS PRINCIPLES

A. INTEGRATED CONFIGURATION AND TECHNICAL CONCERNS

Use FCS and ERS and their energy supply systems, which are DN and TPS, respectively, are the main parts of the SETS. This integrated configuration also includes the RBE and the BESS based on the DC system. To elaborate more, the electricity network configuration of ERS could be a DC-connected or an AC-connected system. AC-connected systems face power quality problems such as inductive voltage drop, voltage or current imbalance, low power factor, and harmonics; therefore, excessive compensating components should be utilized. Furthermore, the neutral sections between the phase rotation blocks cause a speed reduction of trains and arc issues in AC-connected systems. Lastly, expensive installations like booster transformers, autotransformers, or other similar AC installations are the hurdles to their usage. Therefore, employing DC-connected systems is preferable for urban ERSs [1].

The configuration for the electricity network of FCS also could be a DC-connected or an AC-connected system. The AC-connected configuration though beneficial, having a mature background in terms of technology and standards of power electronic devices and also experimental references like Tesla Supercharger and ABB Terra HP [33], is not recommended for such a mentioned integrated framework. The more conversion stages in AC-connected systems between the chargers, BESSs, and DGs increase the complexity and the cost while decreasing the efficiency. Thus, a DC bus, playing the role of an interface, is taken into consideration to simplify electricity collection and delivery. However, utilizing the DC-connected configuration for FCSs has some challenges like galvanic isolation, protection, and metering, which could be met by proposing a transformer, called a solid-state transformer. Further, the mentioned transformer provides the configuration with reasonable circumstances that are compatible with the integration of DGs and ESSs since it would replace both the conventional transformer and AC/DC stage of FCS chargers to create the DC bus [33].

Since DC-connected configuration is preferable for both urban ERS and FCS, the SETS's items can be integrated at the DC level. It is shown in Fig. 1 that TPS and DN are connected to separate DC buses by dedicated step-down transformers and rectifiers; ERS and the DC/DC stage of FCS chargers are also connected to TPS-related and DN-related buses, respectively. The idiosyncrasy of the integrated configuration is the ERS connection to the FCS-related DC bus, unlike the conventional non-integrated configuration. That is, further to the DN, RBE generations with the companion of BESS are going to feed the FCS through the DC bus.

B. OPERATION-AWARE OPTIMIZATION

The integrated configuration showed that the SETS consists of a consumer which is the FCS load and the FCS-ESCH which is a combination of the DN, RBE, and BESS. The aim is to supply the consumer with the minimum cost of investment and operation.

At this stage, to avoid the complexity of interactions among different entities (e.g., ERS, distribution system operators, FCS providers) a holistic approach based on social welfare is considered to find the optimal operation-aware planning for the energy exchanges in SETS and its component sizes. Indeed, this holistic approach would prove that from a social welfare point of view, the integration of ERS and FCS is likely to prevent RBE from wasting and to cut energy obtained by FCS from the DN.

A problem with a detailed set of objectives, constraints, and decision variables for the explained operation-aware optimization model is formulated in section III. To solve the optimization problem, the following assumptions delineate a framework:

1) The time step (t) of the optimization problem is five minutes;

2) The simulated RBE in the form of daily generation profiles is obtained from the ERS simulation described in section IV;
3) The daily profile of FCS power demand as the consumer is known in advance by referencing literature studies ($P^{L}_{d,t}$); In practice, the FCS power demand profile can be obtained by studying the type of EVs as well as the charging behavior of consumers [3];
4) BESS is modeled as a set of electrochemical batteries connected through a converter to the DC link;
5) Since the price of electricity that FCS purchases from DN is different in each season, seasonal price profiles ($\pi^{G}_{s,t}$) are taken into consideration. Besides, the daily profile of the RBE and the FCS load are different on weekdays and weekends. Thus, the profiles of decision variables vary from weekdays to weekends and from season to season.
6) The per-unit prices of BESS, related to its energy capacity (π^{E}_{ESS}), power rating (π^{P}_{ESS}), and operation/maintenance (π^{OM}_{ESS}) are known in advance.
7) The per-unit price of the RBE converter, related to its power rating (π_{Rconv}) is known in advance.
8) The interest rate of the market causes the opportunity cost, considered by multiplying $(1 + DR)^{-y}$ to operation/maintenance costs. This is how their present values are calculated to be added to the investment cost [34].
9) The problem is solved in the GAMS environment on a Windows 10-based system with an Intel(R) Core(TM) i7-6800K CPU 3.40GHz processor in 0.219 seconds, using CPLEX v.12 as the solver [35].

III. OPTIMIZATION MODEL AND SOLUTION ALGORITHM

The operation-aware optimization model of the SETS framework is formulated as an LP problem in this section. The main objective of the optimization model is to maximize social welfare by minimizing the cost of investment and operation:

$$\min_{\psi} C_{IR} + C_{IS} + \sum_{y} (1 + DR)^{-y}.(C_{OG} + C_{OS}) \quad (1)$$

The objective function (1) is the minimization of the overall cost of the SETS includes four terms. Note that the cost of the existing infrastructure of ERS and FCS is not taken into consideration. The first and second terms of the objective function are the investment costs of the RBE converter, and the BESS, respectively. The third and fourth terms are the cost of electricity purchased from DN and the operation/maintenance costs of the BESS over the lifetime duration of the study, respectively. These costs are calculated at the beginning of the lifetime duration of the study. This is why the third and fourth terms are obtained by adding the values of all years together when the annual discount rate is considered; then they are added to the initial investment costs. Consequently, the four terms are calculated by (2-5).

$$C_{IR} = P^{R}_{max}.\pi_{R_{conv}} \quad (2)$$

The investment cost of the RBE converter, which is the interface between the ERS and FCS, is calculated in (2) by multiplying the maximum power flow transmitted from the ERS to FCS, the power rating of the RBE converter, by the per-unit power price. The investment cost of the BESS is obtained in (3).

$$C_{IS} = P_{ESS}.\pi^{P}_{ESS} + E_{ESS}.\pi^{E}_{ESS} \quad (3)$$

The first and second terms, referring to the power rating and energy capacity, respectively, affect the type and price of the BESS individually. Therefore, they are multiplied by their related per-unit prices separately. Equation (4) shows the FCS cost of purchasing electricity from the DN in one year. As mentioned in assumption number 5 in section II, a representative week for each season is chosen to compute the costs of operation.

$$C_{OG} = \sum_{s} q^{w}_{s}.(\sum_{d}\sum_{t} (P^{G}_{s,d,t}.\pi^{G}_{s,d,t}.\Delta t)), \quad \forall s,\ \forall d,\ \forall t \quad (4)$$

The set of decision variables ψ includes the investment cost of the interfacing converter between the ERS and FCS, the investment cost of the BESS, the cost of electricity purchased by FCS from DN, the operation/maintenance cost of the BESS, power flow transmission from the ERS to the FCS, maximum power flow transmission from the ERS to FCS (the power rating (size) of the related RBE converter), the power rating of the BESS and its energy capacity, maximum power flow transmission from the DN to the FCS, BESS discharging and charging power, and finally, the SOC of BESS. It is noted that the items with variable sizes are distinguished by a red color surrounding them in Fig. 1.

According to (4), the weekly purchased electricity is derived from the summations of energy and seasonal price products over the time steps during a week. Consequently, the weekly purchased electricity for each season is multiplied by the number of weeks in the seasons to form the seasonal purchased electricity. Ultimately, the summation of four seasonal purchased electricity forms the yearly purchased electricity.

Equation (5) delineates the costs of BESS operation/maintenance in one year. The first term is obtained by multiplying the energy capacity of the BESS and the per-unit annual cost of its operation/maintenance. The second term presents the cost of BESS residual energy, which is the cost of stored energy differences at the first and final time steps of each day. Considering this cost in the cost function ensures that the difference between the SOC of BESS at the beginning and the end of the day is minimal, and applies the impact of residual energy on the daily cost [36]. In practice, the difference in SOC can be drawn from the grid at the end of each day, and the price of this energy in each season also could be the one at the final time step of the

representative day.

$$C_{\mathrm{OS}} = E_{\mathrm{ESS}}.\pi_{\mathrm{ESS}}^{\mathrm{OM}} + \sum_{s} \mathrm{q}_{s}^{w}.(\sum_{d} (SOC_{s,d,T} - SOC_{s}^{in}).\pi_{s,d,T}^{G}),$$
$$\forall s,\ \forall d \tag{5}$$

The set of constraints (6–12) are binding the objective function (1). Constraint (6) enforces the power balance for the system. Thus, the total of the FCS-ESCH items, including the RBE, BESS, and DN, as the decision variables, should be equal to the FCS load over the time steps.

$$P_{s,d,t}^{\mathrm{G}}.\eta_{\mathrm{G}} + (P_{s,d,t}^{\mathrm{dch}} - P_{s,d,t}^{\mathrm{ch}}).\eta_{\mathrm{ESS}} + P_{s,d,t}^{\mathrm{R}}.\eta_{\mathrm{R}} = P_{d,t}^{\mathrm{L}},$$
$$\forall s,\ \forall d,\ \forall t \tag{6}$$

Constraint (7) models the limit of the DN's power rating which must not be greater than the existing FCS rating.

$$0 \le P_{s,d,t}^{\mathrm{G}} \le P_{\max}^{\mathrm{G}}, \quad \forall s,\ \forall d, \forall t \tag{7}$$

Constraints (8) and (9) limit the power flow from the ERS to FCS. In constraint (8) the power rating of the RBE converter limits this power flow.

$$P_{s,d,t}^{\mathrm{R}} \le P_{\max}^{\mathrm{R}}, \quad \forall s,\ \forall d, \forall t \tag{8}$$

$$P_{s,d,t}^{\mathrm{R}} \le P_{d,t}^{\mathrm{RBE}}, \quad \forall s,\ \forall d, \forall t \tag{9}$$

In constraint (9) the power flow from the ERS to FCS is limited to the amount of the available RBE.

For obtaining available RBE, the power rating of the RBE converter as a limit is applied to the simulated RBE with a time step of 1 second obtained from the ERS simulation since the power flow has instantaneous peaks. Note that the limited RBE is averaged over every 5 minutes to be adapted to the operation-aware optimization model as the available RBE. Accordingly, as the power rating of the RBE converter is a variable, different generation profiles for the available RBE could be derived and inputted into the optimization model as a parameter. This is why a sensitivity analysis of the power rating of the RBE converter and consequently over the generation profiles for the available RBE as a complement to the optimization model is performed to quantify the impact of their changes on the optimal solutions. Ultimately, the optimal solution for this decisive variable (power rating of the RBE converter) is the one at which the objective function of the optimization model, the overall cost of the SETS, is minimal. The set of constraints (10-12) models the BESS.

$$SOC_{s,d,t} = (1-\sigma).SOC_{s,d,t-1} + (P_{s,d,t}^{\mathrm{ch}}.\eta_{ch} - P_{s,d,t}^{\mathrm{dch}}/\eta_{dch})$$
$$.\Delta t, \forall s,\ \forall d,\ \forall t \tag{10}$$

$$(1-\mathrm{DoD}_{\max}).E_{\mathrm{ESS}} \le SOC_{s,d,t} \le (1-\mathrm{DoD}_{\min}).E_{\mathrm{ESS}},$$
$$\forall s,\ \forall d,\ \forall t \tag{11}$$

$$0 \le P_{s,d,t}^{\mathrm{dch}}, P_{s,d,t}^{\mathrm{ch}} \le P_{\mathrm{ESS}}, \quad \forall s,\ \forall d,\ \forall t \tag{12}$$

The optimization variables are defined as:

$$\psi = \left\{ \begin{array}{l} C_{\mathrm{IR}}, C_{\mathrm{IS}}, C_{\mathrm{OG}}, C_{\mathrm{OS}}, P_{s,d,t}^{\mathrm{R}}, P_{\max}^{\mathrm{R}}, P_{\mathrm{ESS}}, \\ E_{\mathrm{ESS}}, P_{s,d,t}^{\mathrm{G}}, P_{s,d,t}^{\mathrm{dch}}, P_{s,d,t}^{\mathrm{ch}}, SOC_{s,d,t} \end{array} \right\}$$

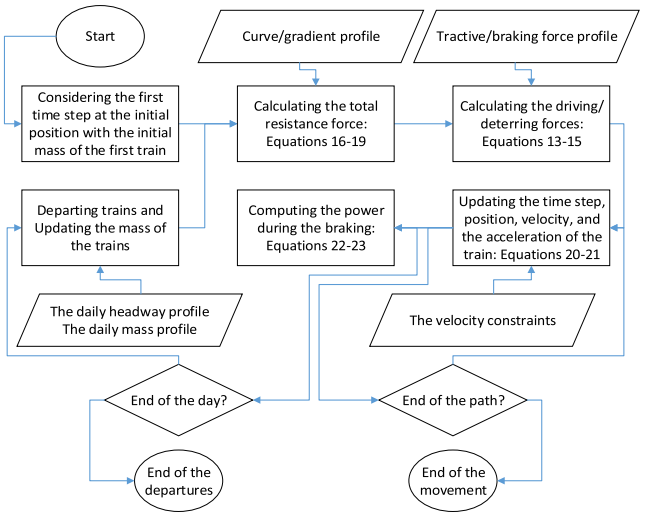

FIGURE 2. ERS simulation flowchart.

The SOC of the BESS at each time step is calculated in constraint (10), which is the sum of the previous SOC, the charging power, and the discharging power with respective efficiencies. Constraint (11) models the operating point limits of the SOC by applying the maximum and minimum depth of discharge. Constraint (12) also models the operating point limits of the BESS power by limiting the charging and discharging power of the BESS to the power rating. It is worth mentioning that since the focus of this study is not on the BESS attributes, advanced constraints like the degradation and the lifetime of the BESS are not taken into account.

IV. ERS MODELING AND SIMULATION

This section presents the ERS generic simulation to determine the RBE's daily profile so that it could be utilized in the operation-aware optimization model of the SETS. The simulation to obtain the RBE generation profile with the time step of 1 second is done in the MATLAB environment on a Windows 10-based system with an Intel(R) Core (TM) i7-6800K CPU 3.40GHz processor.

To begin with, the headway of the trains' departures and the passengers' mass transported on each trip play essential roles in ERS simulation, and it is their daily profiles that delineate how the pattern of the energy exchanges could be. Moreover, specifications of the trains like the tractive and braking forces of motors according to their velocities, aerodynamic attributes, efficiencies, rotating mass factor, and the quantity of the trains in a system, in addition to the specifications of the path like gradient percent and curve radius during the path and velocity constraints are the parameters that are provided for the simulation process.

ERS simulation procedure, which is delineated in the flowchart in Fig. 2, could be explained by investigating a train's movement between two stations, and then it could be generalized to the whole path when other trains also start

departing. Accordingly, there are four stages of a train's movement between stations: acceleration, cruising, coasting, and braking. At the acceleration stage, the driving force, derived by (13), propels the train. The driving force is the net result of the motors' tractive force and the total resistive force interaction. Moreover, the driving force is equal to the product of the train's mass and its acceleration too; this equality helps determine the acceleration to be used in (20-21) to update the position and the velocity of the train at each time step. Note that the mass participating in these equations is the mass of a train and its passengers. Subsequently, the driving force is set to be equal to the total resistive force to create a constant velocity at the cruising stage. Then, the driving force is omitted while only the total resistive force is applied to the train to cause negative acceleration at the coasting stage, which is the neutral mode. Finally, at the braking stage, the deterring force, derived by (14), is applied to the train to stop it at the proper position, which is the next station. The deterring force is the sum of the braking and total resistive force.

$$F_{i,n,x} = TE^{v} - F^{\mathrm{tr}}_{i,n,x} = M^{\mathrm{eff}}_{i,n}.a_{i,n,x}, \quad \forall i,\ \forall n,\ \forall v,\ \forall x \tag{13}$$

$$F_{i,n,x} = F^{v}_{b} - F^{\mathrm{tr}}_{i,n,x} = M^{\mathrm{eff}}_{i,n}.a_{i,n,x}, \quad \forall i,\ \forall n,\ \forall v,\ \forall x \tag{14}$$

Here, $M^{\mathrm{eff}}_{i,n}$ considers the effect of rotation on the mass by a rotation mass factor as formulated in (15).

$$M^{\mathrm{eff}}_{i,n} = M_{i,n}.R, \quad \forall i,\ \forall n \tag{15}$$

The total resistance force is the summation of three forces:

$$F^{\mathrm{tr}}_{i,n,x} = F^{\mathrm{drag}}_{i,n,x} + F^{\mathrm{grad}}_{i,n,x} + F^{\mathrm{p}}_{i,n,x}, \quad \forall i,\ \forall n,\ \forall v,\ \forall x \tag{16}$$

1. Aerodynamic resistive force: occurring because of friction between train and air, and bearing and axles, obtained as follows:

$$F^{\mathrm{drag}}_{i,n,x} = \mathrm{A} + \mathrm{B}.V_{i,n,x} + C.V^{2}_{i,n,x}, \quad \forall i,\ \forall n,\ \forall v,\ \forall x \tag{17}$$

2. Gradient resistive force: occurring because of the horizontal component of the trains' weight, which is calculated as follows:

$$F^{\mathrm{grad}}_{i,n,x} = M^{\mathrm{eff}}_{i,n}.\mathrm{g}.S_{i,n,x}, \quad \forall i,\ \forall n,\ \forall x \tag{18}$$

3. Curvature resistive force: occurring because of centrifugal movement of trains along the curves, obtained as follows:

$$F^{\mathrm{p}}_{i,n,x} = M^{\mathrm{eff}}_{i,n}.\mathrm{g}.\mu_{\mathrm{curve}}.\mathrm{D}/r_{i,n,x}, \quad \forall i,\ \forall n,\ \forall x \tag{19}$$

A, B, C, and D are coefficients, determined experimentally.

The forces for a specific position are obtained as explained. Subsequently, the position and velocity could be updated by (20-21) at each time step to repeat the previous steps for obtaining the forces all over the path.

$$V^{2}_{2_{i,n,x}} - V^{2}_{1_{i,n,x}} = 2.a_{i,n,x}.\Delta x_{i,n,x}, \quad \forall i,\ \forall n,\ \forall v,\ \forall x \tag{20}$$

$$\Delta x_{i,n,x} = 0.5.a_{i,n,x}.i^{2} + a_{i,n,x}.i, \quad \forall i,\ \forall n,\ \forall v,\ \forall x \tag{21}$$

Ultimately, the forces applied to a train all over the path are obtained up to this step. As delineated in Fig. 2, according to the differing mass and headway profiles during the days, other trains start departing in the next step, and the forces applied to all trains all over the path could be obtained by repeating previous steps. These forces are used then to obtain the power interactions. It should be noted that during each day, the power curvature contains positive and negative values, representing power consumption and regeneration in succession. Hence, in (22) summing the products of trains' force and velocity obtains the RBE generation profile in the vicinity of a sample station. The efficiency of the motor and the drive also is considered according to (23).

$$P^{\mathrm{RBE}}_{d,i} = |\sum_{n} F_{i,n,x}.V_{i,n,x}|.\eta, \quad \forall i,\ \forall n,\ \forall x \in st, \forall F_{i,n,x} \leq 0 \tag{22}$$

$$\eta = \eta_{\mathrm{Motor}}.\eta_{\mathrm{Drive}} \tag{23}$$

V. CASE STUDY AND RESULTS

The proposed optimization model and RBE model are applied to a realistic case study here to demonstrate the feasibility and effectiveness of employing SETS to alleviate the setbacks of FCS development. This case study is comprised of a FCS based on reports from the literature, a real ERS, and real prices for components and electricity according to the global scale. The assumptions and the framework for the attributes of these items are explained as follows in parameter properties.

A. PARAMETER PROPERTIES

The sets of data associated with the case study are explained to see how the optimal solutions are going to be derived:

1) The FCS load: Due to the lack of a real local FCS load profile as the case study, it is synthesized as follows. The weekdays and weekend daily profiles of a FCS load reported in [33] are normalized to the sample of a real DC-connected FCS with the rated power of 675 kW, reported in [3] (shown in Fig. 8).

2) RBE generations: Regarding the simulation of the RBE generations, explained in the previous section, the specifications, and parameters of line number 6 of the Tehran Metro transportation system, Tehran, Iran as the real case study are presented in Table 2.

Besides, Fig. 3 (a) shows the tractive and braking forces of trains' motors at each velocity. The case study documents also present the aerodynamic resistive force with a curve shown in Fig. 3 (b). Moreover, the routine headways that could respond to the passenger demand as well as the daily profiles of trains' mass according to passenger demand for both weekdays and weekends are shown in Figs. 3 (c) and 3 (d), respectively. The other datasets related to the case study, including gradient, curve, and speed limits according to the position of the path in addition to the position of stations are provided in [37].

As to the location of the SETS establishment, the second station of Tehran line-6 metro as a sample station is the place near which the FCS is assumed to be located. Hence,

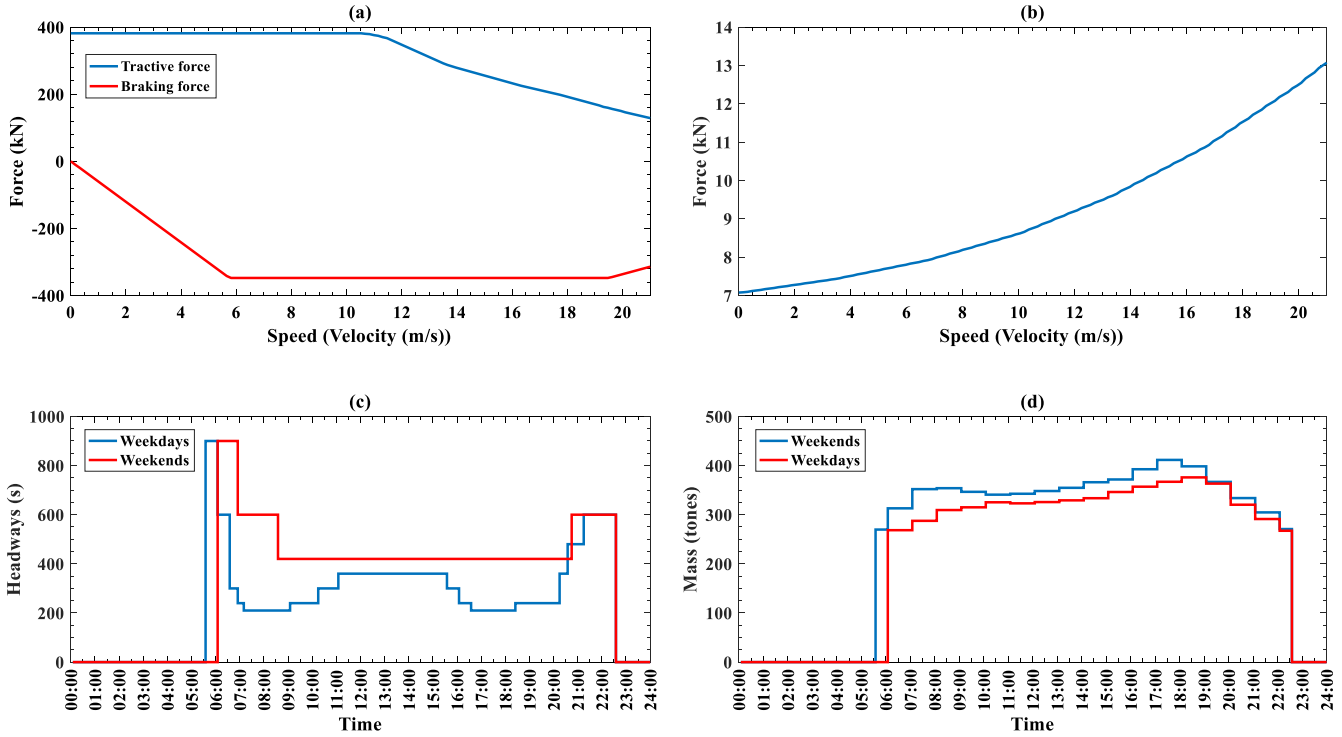

FIGURE 3. Train movement figures. (a) Train tractive/braking forces, (b) Train aerodynamic force, (c) Departure headways, (d) Train mass.

TABLE 2. ERS simulation parameters.

Parameters	Values
Acceleration limit [m/s^2]	-1
Acceleration limit [m/s^2]	+1
η_{Motor}	90%
η_{Drive}	95%
Number of trains on the line	48
Train length [m]	28
Train's empty load [tons]	253.5
Train's AW3 load [tons]	158
R	1.084
μ_{curve}	0.32
ca	7
D	10811.7

by applying the ERS simulation process to the case study, the RBE generation profile in the vicinity of the second station as a result of trains' braking in the vicinity could be derived with the time step of 1 second.

The amount of available RBE, which could contribute to the FCS-ESCH, is a stochastic variable that depends on several uncertain factors. To name some of them, the availability of other accelerating trains that could reuse the RBE while a train is braking, delays in braking time, the reaction of drivers, etc. could be mentioned. In the optimization model, we have not considered such uncertainties. Instead, to consider their effect, we have considered different generation profiles for the available RBE according to different power ratings for the converter between the ERS and FCS. Thus, the sensitivity analysis over the power rating of the RBE converter and consequently over the generation profiles for the available RBE is performed both to determine the optimal solution for the power rating of the RBE converter as explained in section III and to meet the impact of uncertainties as mentioned here. Accordingly, to obtain the available RBE, as explained in section III, it is indispensable to apply the power rating of the RBE converter to the simulated RBE generations as a limit when the time step is 1 second to meet the instantaneous RBE peaks.

Afterward, it needs to be averaged over every 5 minutes to be adapted to the operation-aware optimization model.

Ultimately, the case study generation profiles for the available RBE for different power ratings of the RBE converter over which the sensitivity analysis has been performed, are shown in Fig. 4. The optimization problem, therefore, will consider these generation profiles as parameter datasets for the available RBE.

3) The investment costs of the BESS: The per-unit price of the BESS energy capacity is 132$/kWh at the time in which the case study is being analyzed and it is anticipated that it is going to be decreased in the next years. Companies like Renault and Ford have publicly announced targets of 80$/kWh by 2030 [38]. Therefore, a sensitivity analysis is performed over the price of the per-unit price of the BESS energy capacity to quantify its impact on the optimal solutions.

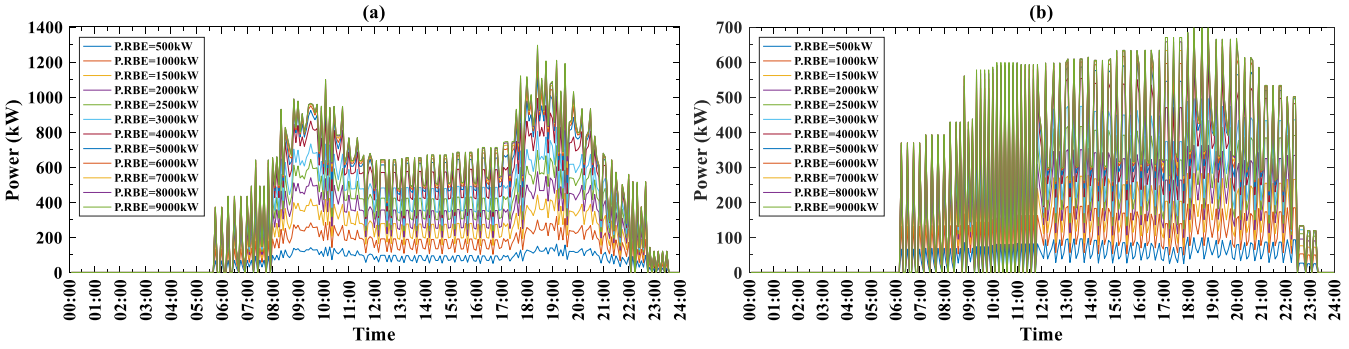

FIGURE 4. Available RBE generations for different power ratings of RBE converter: (a) Weekdays, (b) Weekends.

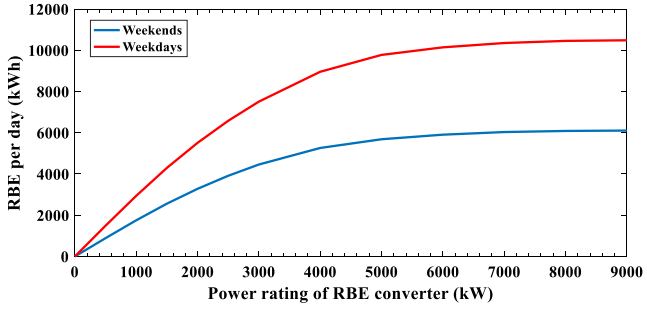

FIGURE 5. Whole RBE generations during a day.

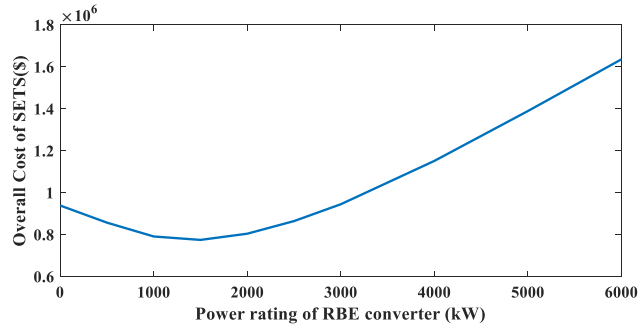

FIGURE 6. The overall cost of SETS.

TABLE 3. Specifications of proposed sets.

Parameters	Values
Lifetime duration of the study (years)	30
Power-related cost of BESS and RBE converter (kW)	250
Operation and maintenance cost of BESS ($/kW year)	35
BESS and RBE converter's efficiency	0.9
BESS round-trip efficiency	0.8
DN converter efficiency	0.9

4) Other specifications: The general specifications and assumptions for the attributes of the case study are presented in Table 3.

Up to this step, the case study has been presented thoroughly. The next step is performing the sensitivity analyses by which the optimal solutions could be analyzed in the related subsection as follows. Accordingly, the range of sensitivity analysis over the per-unit price of the BESS energy capacity is from 132$/kWh down to 80$/kWh as mentioned in the parameter properties subsection; however, to explore the range of sensitivity analysis over the power rating of the RBE converter, the whole energy that could be transmitted to the FCS during a day when the power rating of the RBE converter has different values should be investigated. In this regard, the power rating of the RBE converter over which the daily RBE generation does not increase represents the range of related sensitivity analysis since the greater ratings are not likely to change optimal solutions. This range is 6000kW as shown in Fig. 5.

B. SENSITIVITY ANALYSES

Here the sensitivity analyses over the power rating of the RBE converter and the per-unit price of the BESS energy capacity are performed. The aim of performing sensitivity analyses is to investigate their impacts on the objective function of the optimization problem which is the SETS overall cost during the years, the BESS energy capacity, and the BESS power rating. To commence, sensitivity analysis of the power rating of the RBE converter affects the optimal solution of the objective function. Fig. 6 indicates that the SETS overall cost is 938339$ when there is no available RBE to feed the FCS-ESCH. However, with the rise in the power rating of the RBE converter and consequently in available RBE, the SETS overall cost has a decreasing trend until it reaches its minimum value when the power rating of the RBE converter is 1500kW.

This is the overall optimum solution for the objective function of the LP problem which is 774373$. Hence, employing the SETS causes a reduction of 17.47% in the overall cost compared to the conventional system. Afterward, following the rise in the power rating of the RBE converter, it can be seen that the SETS overall cost has an increasing trend. This increasing trend is suggestive of the fact that, with the growth in the power rating of the converter to more than 1500 kW, although more free-of-charge RBE generation is going to be available, the cost of the converter is going to be so high that the free-of-charge RBE generations could not

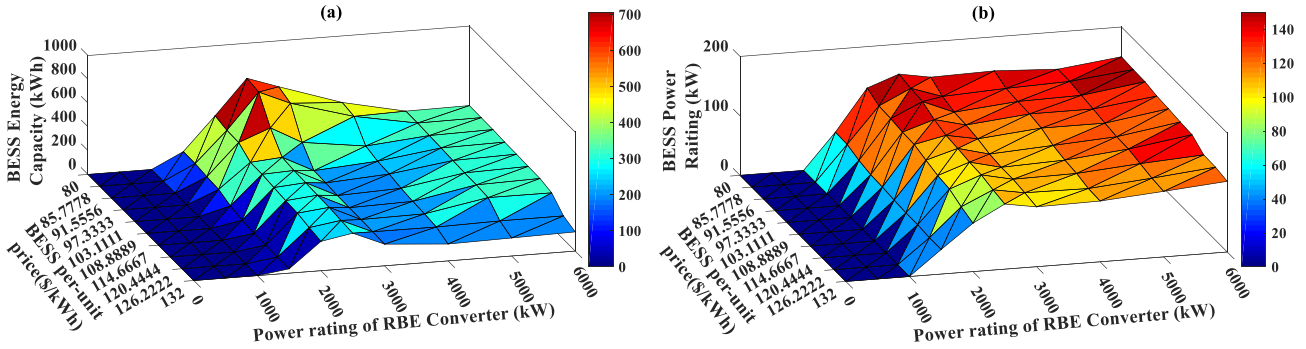

FIGURE 7. Optimal solutions through the sensitivity analyses (a) for BESS energy capacity (b) for BESS power rating.

compensate for the impact of converter cost on the SETS overall cost. Nonetheless, unlike the sensitivity analysis over the sensitivity analysis over the power rating of the RBE converter, the sensitivity analysis over the per-unit price of the BESS energy capacity has a negligible impact on the objective function of the LP problem which is the SETS overall cost. For example, for the RBE converter power rating of 6000 kW, the SETS overall costs are 1635643$ and 1620341$ when the per-unit price of the BESS energy capacities are 132$/kWh and 80$/kWh, respectively.

For the RBE converter power rating of 1500 kW, the SETS overall costs are 774373$ and 770574$ when the per-unit price of the BESS energy capacities are 132$/kWh and 80$/kWh, respectively. This means that with the decrease in the per-unit price of the BESS energy capacity from 132$/kWh down to 80$/kWh in the future, the implementation of the SETS is not merely more feasible and interesting compared to today's per-unit price as the SETS overall cost will decrease for just %0.91 and %0.49 for RBE converter power rating of 6000 kW and 1500 kW, respectively. In addition to the objective function of the LP problem, the behavior of the BESS energy capacity and power rating when the sensitivity analyses are performed are investigated here. Fig. 7 illustrates the impact of changes in both the power rating of the RBE converter and the per-unit price of the BESS energy capacity at the same time.

Fig. 7 (a) shows the optimal solutions for the BESS energy capacity through sensitivity analyses. As to the effect of the power rating of the RBE converter, when it increases, the BESS energy capacity has an increasing trend until it reaches its apex at about 700 kWh when the power rating of the RBE converter is around 2500 kW, and the per-unit price of the BESS energy capacity is 80$/kWh, and then after a short decreasing trend, it remains relatively stable. This could be interpreted by the fact that before the power rating of the RBE converter reaches 2500 kW, there is a lack of sufficient available RBE to meet the load demand, and the BESS should manage to do that, but with the growth of the available RBE, the need for BESS diminished. Note that although the BESS energy capacity is maximum when the power rating of the RBE converter is around 2500 kW, the overall optimum cost of the SETS happens at the other point since there is no linear relation between them. Besides, it is inferred from Fig. 7 (a) that BESS energy capacity has generally an increasing trend when the per-unit price decreases since the BESS with the lower per-unit price for the energy capacity enables the optimization model to choose the BESS with higher energy capacity.

Fig. 7 (b) depicts the optimal solutions for the BESS power rating through the sensitivity analyses, which is indicative of the power rating of the BESS converter. It is indicated that with the growth of the power rating of the RBE converter, this variable steeply increases for all per-unit prices, reaching a plateau of around 150 kW when the power rating of the RBE converter is approximately 2500 kW. This is a behavior similar to what BESS energy capacity shows. Therefore, it could be mentioned that before a certain power rating of the RBE converter which is 2500 kW, the power flow from the ERS is not enough to feed the FCS, and BESS tends to increase its contribution whereas with the growth of the available RBE more than 2500 kW, the need for BESS is obviated. It is noted that there is a gently rising trend for this variable due to the reduction in the per-unit prices of BESS energy capacity since the optimization model tends to choose a higher power rating for the BESS when the per-unit price becomes lower. The inclination of the optimization model to prefer RBE to BESS in the FCS-ESCH ensues from the distinction that could be drawn between their costs. That is, employing RBE depends on paying just for its converter while its generation is free of charge; however, utilizing BESS relies on paying both for the converter and the energy capacity.

With respect to the energy capacity and power rating of the BESS when the power rating of the RBE converter has its optimal value which is 1500kW according to Fig. 6, their values start respectively from 36 kWh and 40 kW for the per-unit price of 132 $/kWh and finish at 130 kWh and 60 kW for the per-unit price of 80 $/kWh.

After the investigation into the optimal solution trends through the sensitivity analyses, the discussions about how the SETS can help DN to respond to the FCS demand optimally are done as follows. In the following discussions, the energy exchanges, and the impact of electricity prices

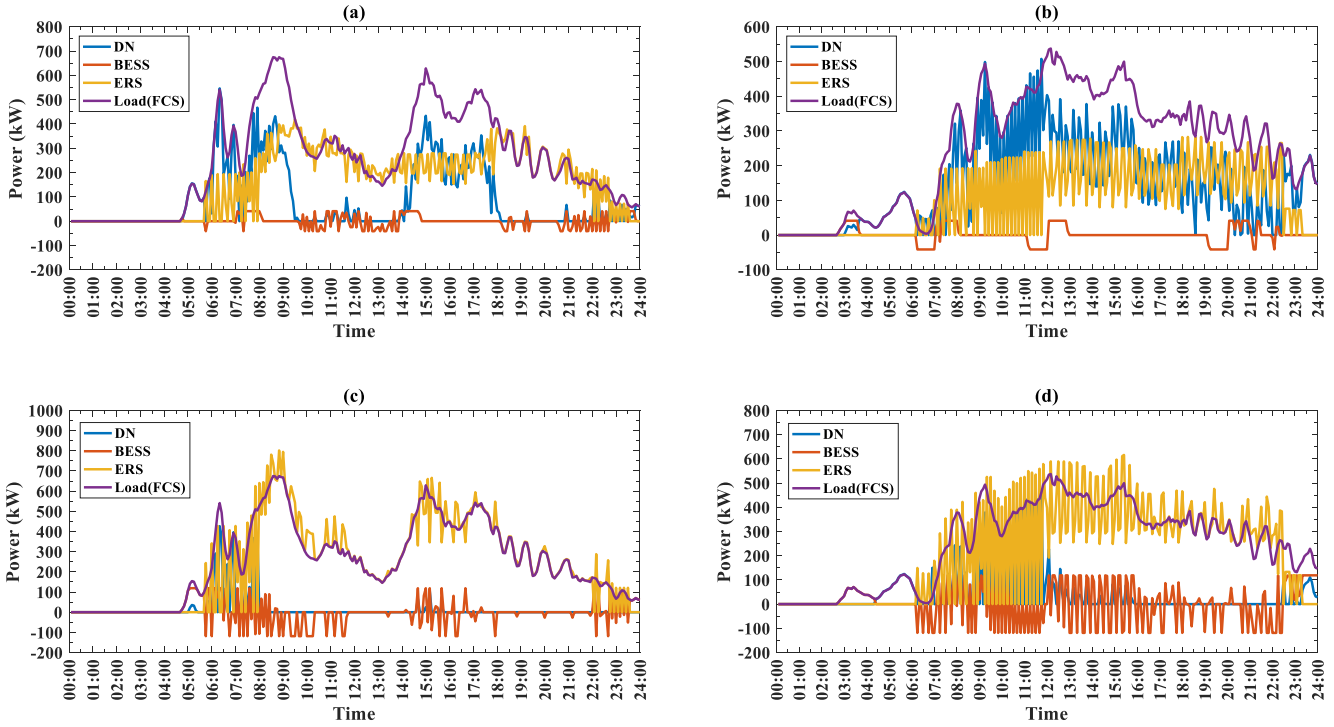

FIGURE 8. Power balance in summer – power rating of RBE converter (Load is FCS): (a) 1500 kW (Weekdays), (b) 1500 kW (Weekends), (c) 6000 kW (Weekdays), (d):6000 kW (Weekends).

on purchased electricity from DN are investigated. These numerical results of optimal solutions vary according to the different power ratings of the RBE converter. Nevertheless, the two ratings leading to distinguished optimal solutions with the current per-unit price of the BESS energy capacity (132 $/kWh) are the focus here. One of them is the one at which the objective function has been optimized (1500kW) and another is the one over which the RBE generation during the days does not increase (6000 kW) (Fig. 5).

C. ENERGY EXCHANGES

The power balance for the two power ratings of the RBE converter during the sample days of a sample season, as shown in Fig. 8, is considered here to investigate the effectiveness of the SETS. With respect to power interactions, it can be inferred from Fig. 8 that the optimal power flow from ERS accompanied by the BESS could feasibly contribute to FCS-ESCH. It is shown that with the participation of RBE and BESS, the peak power demand from the DN is reduced from 675 kW down to almost 500 kW and 400 kW when the power rating of the RBE converter is 1500kW and 6000 kW, respectively.

To conduct more surveys Figs. 8 (a, b) show that when the power rating of the RBE converter is 1500kW, the RBE covers about %66 and %42 of daily required energy in FCS-ESCH on weekdays and weekends, respectively. Thus, %34 (weekdays) and %58 (weekends) of daily required energy in FCS-ESCH is acquired from the DN and BESS.

Nevertheless, when the power rating of the RBE converter is 6000 kW, as shown in Figs. 8 (c, d), due to the increase in the amount of available RBE which makes it nearly sufficient to supply the whole load with the help of the BESS, DN participation in the FCS-ESCH has nearly faded at least on weekdays. That is, %95 and %84 of daily required energy in FCS-ESCH on weekdays and weekends, respectively, is provided by the RBE.

Thus, the more available RBE could be, the more the burden on the DN could be reduced. However, the compromise that shows to what extent reducing the burden on DN is worth increasing the power rating of the RBE converter for more available RBE has been forged by the optimization model and shown in the last subsection. The optimal solutions are affected not only by striking a compromise between the free-of-charge RBE with a payable converter and electricity purchased from DN but also by the difference in prices of electricity purchased from the DN during the hours of the day. Therefore, the impact of the difference in prices of electricity purchased from the DN is also surveyed as follows.

D. PURCHASED ELECTRICITY FROM DN–THE COMPARISON BETWEEN THE SETS AND CONVENTIONAL SYSTEM

The profiles of the prices, power demand from the DN, and load for the seasons during the days are indicated in Figs. 9-12 to investigate the impact of changes in electricity prices on optimal solutions. Besides, these figures have highlighted the differences between the load that used to be completely supplied by the DN in the conventional system and the power demand from the DN in the SETS.

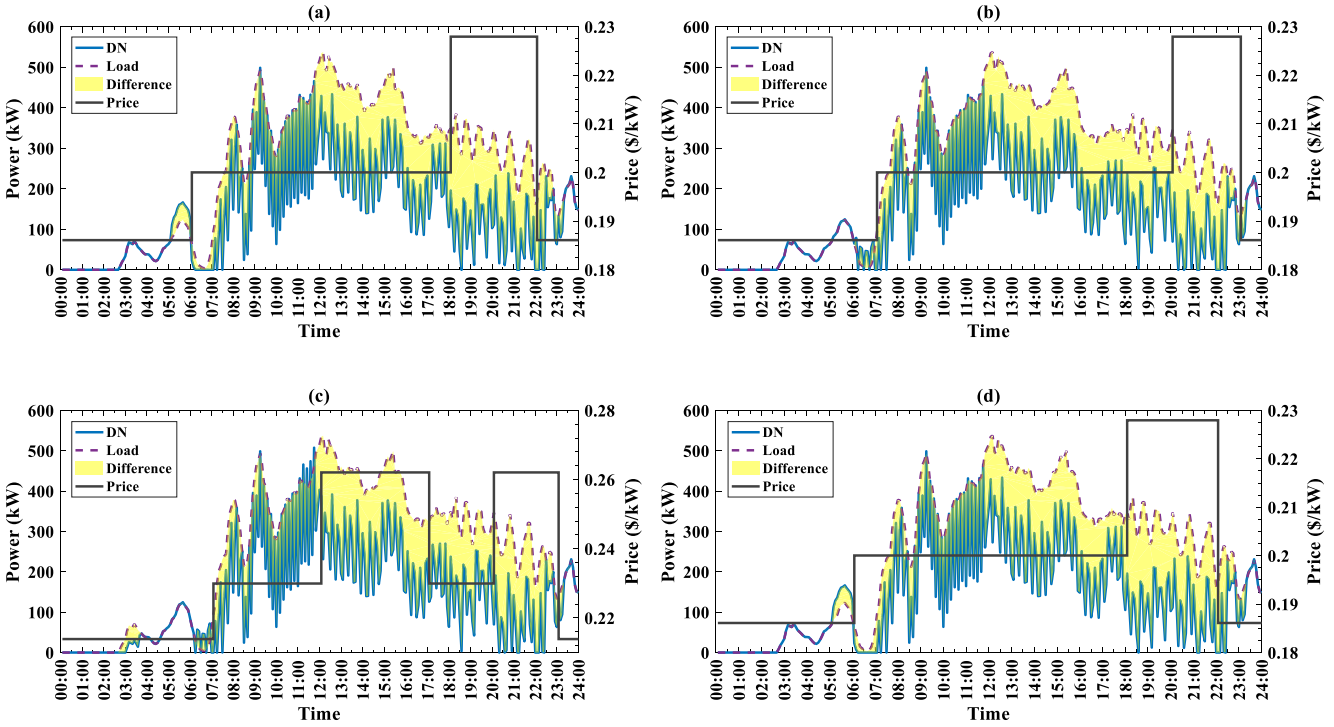

FIGURE 9. Power demand – Weekends - power rating of RBE converter: 1500 kW. (a) Winter, (b) Spring, (c) Summer, (d) Autumn.

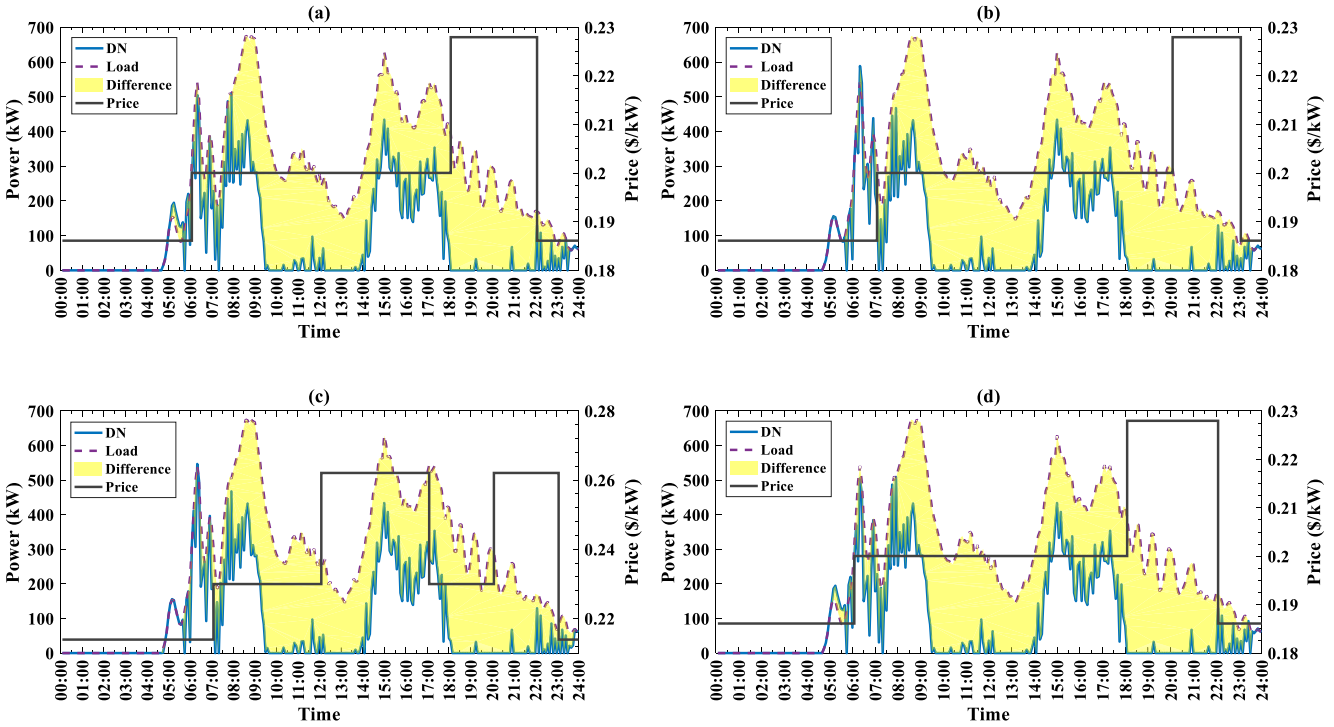

FIGURE 10. Power demand – Weekdays - power rating of RBE converter: 1500 kW (a) Winter, (b) Spring, (c) Summer, (d) Autumn.

According to Figs. 9 and 10, related to results of when the power rating of the RBE converter is 1500kW, the daily required energy in FCS-ESCH for the SETS is %59 and %35 of that energy for the conventional system on weekdays and weekends, respectively.

Furthermore, According to Figs. 11 and 12, related to results of when the power rating of the RBE converter is 6000 kW, the daily required energy in FCS-ESCH for the SETS is about %17 and %5 of that energy for the conventional system on weekdays and weekends, respectively.

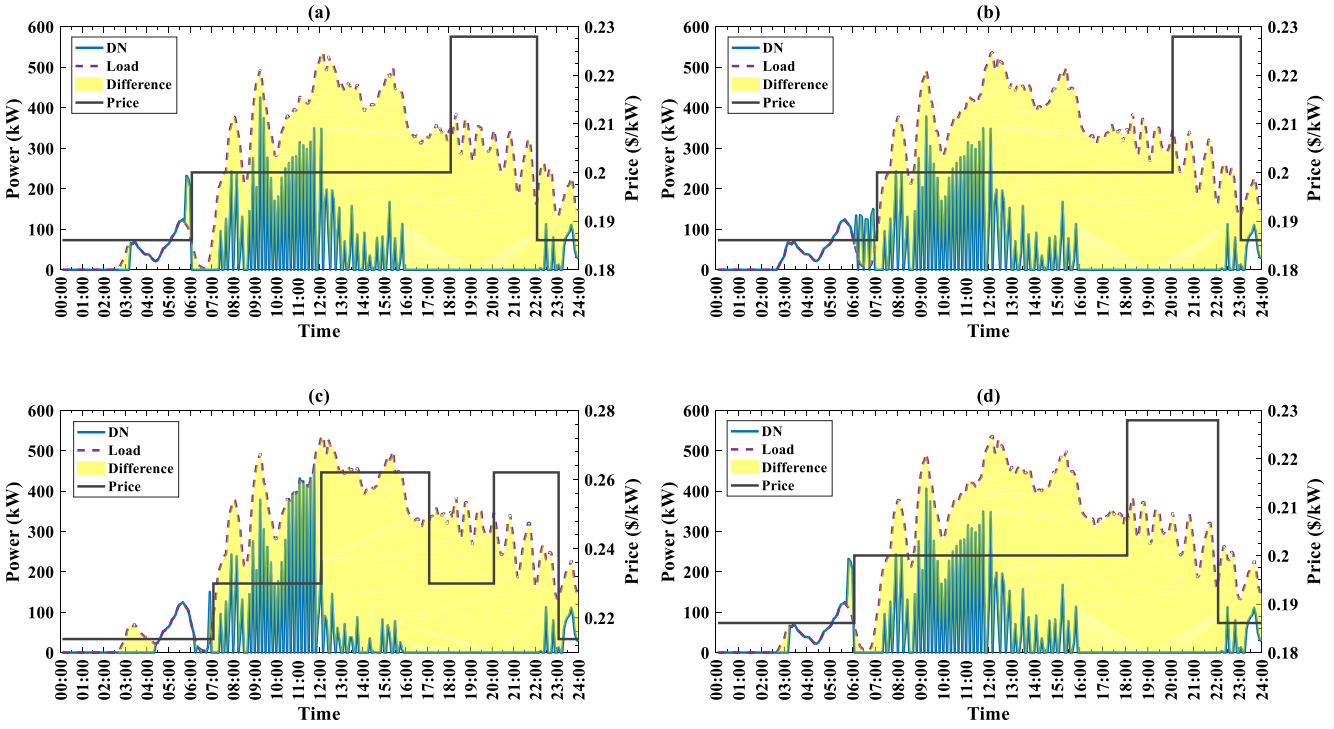

FIGURE 11. Power demand – Weekends - power rating of RBE converter:6000 kW. (a) Winter, (b) Spring, (c) Summer, (d) Autumn.

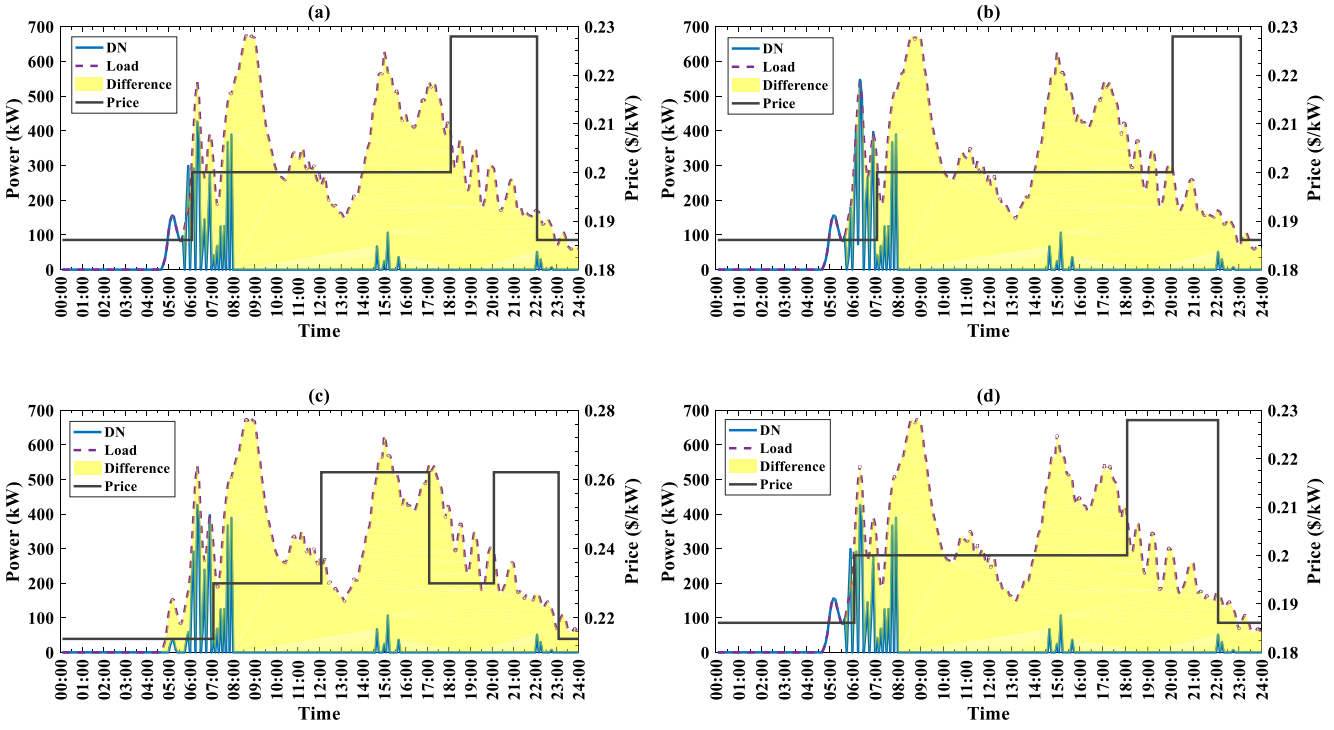

FIGURE 12. Power demand – Weekdays - power rating of RBE converter:6000kW. (a) Winter, (b) Spring, (c) Summer, (d) Autumn.

These differences are indicative of the amount of electricity that is provided by the RBE with the help of the BESS instead of purchasing from the DN and time shifts in purchasing electricity.

To elaborate more, the differences are not just due to the free-of-charge available RBE accompanied by the BESS playing a role in FCS-ESCH, and the different prices of the electricity during the hours of a day could also be a factor for such differences as purchasing during the times of lower prices for using when the prices are higher may be worth paying for BESS for storing.

For example, it could be seen in Figs. 9 (a), 9 (d), 10 (a), and 10 (d), that between 5 o'clock and 6 o'clock over which the electricity price is lower, the SETS tends to purchase electricity more than the load demand to store in the BESS, and then, during the peak power demand, the purchased electricity from the DN is less than the load while the RBE and the BESS are going to compensate for the unpurchased electricity. Thus, the SETS could ease the burden on the DN in terms of both the whole energy and the peak power demand.

By increasing the power ratings of the RBE converter, the available RBE rises, and the difference between the demand and the purchased electricity, as a result, will increase especially at peak times with higher prices. Accordingly, the differences in Figs. 9-10, demonstrating the profiles of when the power rating of the RBE converter is 1500kW, show that the SETS has just damped the power demands moderately, whereas Figs. 11-12, showing profiles of when the power rating of the RBE converter is 6000kW, clear that the power demand from the DN tends to reach zero value.

Note that the electricity prices in Iran are normalized to the standard range which is common throughout the world and the subsidy offered by the local government on electricity is not taken into consideration. Having the same scale for the electricity prices and the investment, operation, and maintenance costs of the SETS makes accurate analyses possible.

VI. SUMMARY AND CONCLUSION

This study proposed a promising strategy to utilize unused braking energy of trains combined with a BESS to supply EV charging stations seeking to notably mitigate the peak power demand of FCSs.

Accordingly, an operation-aware optimization model for the SETS was developed to proceed with energy exchange planning together with proposing optimal solutions for the power rating and energy capacity of BESS and the power rating of the interfacing converter. A generic model for RBE and consequently a set of generation profiles according to different power ratings of the available RBE were obtained to be inputted into the optimization model. The model was applied to a real case study, and numerical results were obtained that proved the viability and efficacy of the SETS. The sensitivity analyses over the per-unit price of the BESS energy capacity and the power rating of the interfacing converter were done and examined their impacts on the optimal solutions.

The results have indicated that different RBE generations according to different power ratings of the RBE converter could viably and optimally participate in FCS-ESCH. Analyzing energy exchanges and electricity prices reveals that maximizing free RBE generation aligns with SETS' goal of reducing peak power demand from the grid. The results also emphasize the importance of strategically timing electricity purchases to avoid higher costs. The sensitivity analysis indicated that the RBE generator should not exceed a power rating of 1500 kW, as this is the optimal rating for minimizing the overall cost of the SETS. It is found that the overall cost of the SETS in this proposed optimum solution is lower than the conventional system by about 17.47%. Meanwhile, it is demonstrated that incorporating BESS is beneficial for FCS-ESCH even when the per-unit price of BESS energy capacity is 132 $/kWh while this price has a decreasing trend. As the energy capacity and power rating of BESS increase as the price decreases, they reach a peak at 700 kWh and 150 kW, respectively, when the RBE converter is around 2500 kW and the BESS price is 80 $/kW. In contrast, when the RBE converter is at its optimum and the BESS price is 132 $/kW, the BESS size is smaller at 36 kWh and 40 kW. This highlights that a moderate-sized BESS can be effective in the optimization model. Accordingly, it is demonstrated that ERS and BESS integration reduces peak demand from 675 kW to about 500 kW.

The study conducted a mathematical feasibility assessment, and its conclusions are contingent on specific assumptions, namely, understanding real-time ERS operations and simplifying BESS constraints related to factors like degradation and lifespan. Consequently, future endeavors could aim to achieve optimal planning, accounting for the impact of real-time uncertainties in ERS operations while also incorporating advanced constraints related to the BESS. Moreover, studying the integration of photovoltaic generations in the SETS is the scope of future work since they are likely to contribute positively to FCS-ESCH.

REFERENCES

[1] M. Brenna, F. Foiadelli, and H. J. Kaleybar, "The evolution of railway power supply systems toward smart microgrids: The concept of the energy hub and integration of distributed energy resources," *IEEE Electrific. Mag.*, vol. 8, no. 1, pp. 12–23, Mar. 2020, doi: 10.1109/MELE.2019.2962886.

[2] F. Kehagia, "Sustainable mobility," in *City Networks* (Springer Optimization and Its Applications), vol. 128. Berlin, Germany: Springer, 2017, pp. 99–119.

[3] S. Negarestani, M. Fotuhi-Firuzabad, M. Rastegar, and A. Rajabi-Ghahnavieh, "Optimal sizing of storage system in a fast charging station for plug-in hybrid electric vehicles," *IEEE Trans. Transport. Electrific.*, vol. 2, no. 4, pp. 443–453, Dec. 2016, doi: 10.1109/TTE.2016.2559165.

[4] G. Joos, M. de Freige, and M. Dubois, "Design and simulation of a fast charging station for PHEV/EV batteries," in *Proc. IEEE Electr. Power Energy Conf.*, Aug. 2010, pp. 1–5, doi: 10.1109/EPEC.2010.5697250.

[5] S. Srdic and S. Lukic, "Toward extreme fast charging: Challenges and opportunities in directly connecting to medium-voltage line," *IEEE Electrific. Mag.*, vol. 7, no. 1, pp. 22–31, Mar. 2019, doi: 10.1109/MELE.2018.2889547.

[6] J. A. Domínguez-Navarro, R. Dufo-López, J. M. Yusta-Loyo, J. S. Artal-Sevil, and J. L. Bernal-Agustín, "Design of an electric vehicle fast-charging station with integration of renewable energy and storage systems," *Int. J. Electr. Power Energy Syst.*, vol. 105, pp. 46–58, Feb. 2019, doi: 10.1016/j.ijepes.2018.08.001.

[7] W. Khan, F. Ahmad, and M. S. Alam, "Fast EV charging station integration with grid ensuring optimal and quality power exchange," *Eng. Sci. Technol., Int. J.*, vol. 22, no. 1, pp. 143–152, Feb. 2019, doi: 10.1016/j.jestch.2018.08.005.

[8] S. Afshar, P. Macedo, F. Mohamed, and V. Disfani, "Mobile charging stations for electric vehicles—A review," *Renew. Sustain. Energy Rev.*, vol. 152, Dec. 2021, Art. no. 111654, doi: 10.1016/j.rser.2021.111654.

[9] H. Saboori, S. Jadid, and M. Savaghebi, "Optimal management of mobile battery energy storage as a self-driving, self-powered and movable charging station to promote electric vehicle adoption," *Energies*, vol. 14, no. 3, p. 736, Jan. 2021, doi: 10.3390/en14030736.

[10] L. Gebhardt, D. Krajzewicz, R. Oostendorp, M. Goletz, K. Greger, M. Klötzke, P. Wagner, and D. Heinrichs, "Intermodal urban mobility: Users, uses, and use cases," *Transp. Res. Proc.*, vol. 14, pp. 1183–1192, Dec. 2016, doi: 10.1016/j.trpro.2016.05.189.

[11] H. J. Kaleybar, M. Brenna, F. Foiadelli, S. S. Fazel, and D. Zaninelli, "Power quality phenomena in electric railway power supply systems: An exhaustive framework and classification," *Energies*, vol. 13, no. 24, p. 6662, Dec. 2020, doi: 10.3390/en13246662.

[12] M. Bozorg, A. Ahmadi-Khatir, and R. Cherkaoui, "Developing offer curves for an electric railway company in reserve markets based on robust energy and reserve scheduling," *IEEE Trans. Power Syst.*, vol. 31, no. 4, pp. 2609–2620, Jul. 2016, doi: 10.1109/TPWRS.2015.2485938.

[13] E. Lakervi and E. J. Holmes, *Electricity Distribution Network Design*, P. Peregrinus, Ed. London, U.K.: IEI, 1995. [Online]. Available: http://books.google.com/books?id=mudSAAAAMAAJ

[14] J. Deng, J. Shi, Y. Liu, and Y. Tang, "Application of a hybrid energy storage system in the fast charging station of electric vehicles," *IET Gener., Transmiss. Distrib.*, vol. 10, no. 4, pp. 1092–1097, Mar. 2016, doi: 10.1049/iet-gtd.2015.0110.

[15] D. Sbordone, I. Bertini, B. Di Pietra, M. C. Falvo, A. Genovese, and L. Martirano, "EV fast charging stations and energy storage technologies: A real implementation in the smart micro grid paradigm," *Electr. Power Syst. Res.*, vol. 120, pp. 96–108, Mar. 2015, doi: 10.1016/j.epsr.2014.07.033.

[16] N. Machiels, N. Leemput, F. Geth, J. Van Roy, J. Büscher, and J. Driesen, "Design criteria for electric vehicle fast charge infrastructure based on Flemish mobility behavior," *IEEE Trans. Smart Grid*, vol. 5, no. 1, pp. 320–327, Jan. 2014, doi: 10.1109/TSG.2013.2278723.

[17] L. Yang and H. Ribberink, "Investigation of the potential to improve DC fast charging station economics by integrating photovoltaic power generation and/or local battery energy storage system," *Energy*, vol. 167, pp. 246–259, Jan. 2019, doi: 10.1016/j.energy.2018.10.147.

[18] S. Afshar, Z. K. Pecenak, M. Barati, and V. Disfani, "Mobile charging stations for EV charging management in urban areas: A case study in Chattanooga," *Appl. Energy*, vol. 325, Nov. 2022, Art. no. 119901, doi: 10.1016/j.apenergy.2022.119901.

[19] *DC Mobile EV Charging Stations*. Accessed: Sep. 29, 2022. [Online]. Available: https://www.power-sonic.com/mobile-ev-charging-stations/

[20] *Volkswagen Lets its Charging Robots Loose*. Accessed: Sep. 29, 2022. [Online]. Available: https://www.volkswagenag.com/en/news/stories/2019/12/volkswagen-lets-its-charging-robots-loose.html

[21] M. Khodaparastan, A. A. Mohamed, and W. Brandauer, "Recuperation of regenerative braking energy in electric rail transit systems," *IEEE Trans. Intell. Transp. Syst.*, vol. 20, no. 8, pp. 2831–2847, Aug. 2019, doi: 10.1109/TITS.2018.2886809.

[22] M. C. Falvo, R. Lamedica, R. Bartoni, and G. Maranzano, "Energy management in metro-transit systems: An innovative proposal toward an integrated and sustainable urban mobility system including plug-in electric vehicles," *Electr. Power Syst. Res.*, vol. 81, no. 12, pp. 2127–2138, Dec. 2011, doi: 10.1016/j.epsr.2011.08.004.

[23] Y. Jiang, J. Liu, W. Tian, M. Shahidehpour, and M. Krishnamurthy, "Energy harvesting for the electrification of railway stations: Getting a charge from the regenerative braking of trains," *IEEE Electrific. Mag.*, vol. 2, no. 3, pp. 39–48, Sep. 2014, doi: 10.1109/MELE.2014.2333561.

[24] S. Nasr, M. Iordache, and M. Petit, "Smart micro-grid integration in DC railway systems," in *Proc. IEEE PES Innov. Smart Grid Technol., Eur.*, Oct. 2014, pp. 1–6, doi: 10.1109/ISGTEurope.2014.7028913.

[25] M. Brenna, F. Foiadelli, H. J. Kaleybar, and S. S. Fazel, "Smart electric railway substation using local energy hub based multi-port railway power flow controller," in *Proc. IEEE Vehicle Power Propuls. Conf. (VPPC)*, Oct. 2019, pp. 1–6, doi: 10.1109/VPPC46532.2019.8952414.

[26] A. González-Gil, R. Palacin, P. Batty, and J. P. Powell, "A systems approach to reduce urban rail energy consumption," *Energy Convers. Manage.*, vol. 80, pp. 509–524, Apr. 2014, doi: 10.1016/j.enconman.2014.01.060.

[27] T. Zhang, E. E. F. Ballantyne, and D. A. Stone, "Fully integrated EV energy storage using transport infrastructure," in *Proc. Int. Conf. Clean Electr. Power (ICCEP)*, Jul. 2019, pp. 337–344, doi: 10.1109/ICCEP.2019.8890133.

[28] M. Stieneker, B. J. Mortimer, A. Hinz, A. Müller-Hellmann, and R. W. De Doncker, "MVDC distribution grids for electric vehicle fast-charging infrastructure," in *Proc. Int. Power Electron. Conf. (IPEC-Niigata ECCE Asia)*, May 2018, pp. 598–606, doi: 10.23919/IPEC.2018.8507594.

[29] A. Fernandez-Rodriguez, A. Fernandez-Cardador, A. De Santiago-Laporte, C. Rodriguez-Sanchez, A. P. Cucala, A. J. Lopez-Lopez, and R. R. Pecharroman, "Charging electric vehicles using regenerated energy from urban railways," in *Proc. IEEE Vehicle Power Propuls. Conf. (VPPC)*, Dec. 2017, pp. 1–6, doi: 10.1109/VPPC.2017.8330998.

[30] A. Çiçek, I. Sengör, S. Güner, F. Karakus, A. K. Erenoglu, O. Erdinç, M. Shafie-Khah, and J. P. S. Catalão, "Integrated rail system and EV parking lot operation with regenerative braking energy, energy storage system and PV availability," *IEEE Trans. Smart Grid*, vol. 13, no. 4, pp. 3049–3058, Jul. 2022, doi: 10.1109/TSG.2022.3163343.

[31] F. Karakuş, A. Çiçek, and O. Erdinç, "Integration of electric vehicle parking lots into railway network considering line losses: A case study of Istanbul M1 metro line," *J. Energy Storage*, vol. 63, Jul. 2023, Art. no. 107101, doi: 10.1016/j.est.2023.107101.

[32] H. Krueger, D. Fletcher, and A. Cruden, "Vehicle-to-grid (V2G) as line-side energy storage for support of DC-powered electric railway systems," *J. Rail Transp. Planning Manage.*, vol. 19, Sep. 2021, Art. no. 100263, doi: 10.1016/j.jrtpm.2021.100263.

[33] H. Tu, H. Feng, S. Srdic, and S. Lukic, "Extreme fast charging of electric vehicles: A technology overview," *IEEE Trans. Transport. Electrific.*, vol. 5, no. 4, pp. 861–878, Dec. 2019, doi: 10.1109/TTE.2019.2958709.

[34] E. Hajipour, M. Bozorg, and M. Fotuhi-Firuzabad, "Stochastic capacity expansion planning of remote microgrids with wind farms and energy storage," *IEEE Trans. Sustain. Energy*, vol. 6, no. 2, pp. 491–498, Apr. 2015, doi: 10.1109/TSTE.2014.2376356.

[35] *V12.1 User's Manual for CPLEX*, document 46, Int. Bus. Mach. Corp., Armonk, NY, USA, 2009, p. 157.

[36] H. Ding, P. Pinson, Z. Hu, and Y. Song, "Optimal offering and operating strategies for wind-storage systems with linear decision rules," *IEEE Trans. Power Syst.*, vol. 31, no. 6, pp. 4755–4764, Nov. 2016, doi: 10.1109/TPWRS.2016.2521177.

[37] S. N. Larijani, *Dataset*. Accessed: Jul. 27, 2023. [Online]. Available: https://github.com/sepehrnajafi/SETS.git

[38] V. Henze. (2021). *Batteries For Electric Cars Speed Toward a Tipping Point*. BloombergNEF. [Online]. Available: https://about.bnef.com/blog/battery-pack-prices-fall-to-an-average-of-132-kwh-but-rising-commodity-prices-start-to-bite/#: :text=For battery electric vehicle (BEV),of the total pack price

SEPEHR NAJAFI LARIJANI received the master's degree in electrical engineering from the Iran University of Science and Technology, in 2017, where he is currently pursuing the Ph.D. degree. His research interests include the electricity market, electric transportation systems, electric railways, renewable energy sources, energy storage systems, and optimization.

SEYED SAEED FAZEL was born in Iran, in 1966. He received the M.Sc. degree in electrical engineering from the Iran University of Science and Technology, Tehran, Iran, in 1993, and the Ph.D. degree in electrical engineering from the Berlin University of Technology, Germany, in 2007. He spent four years (1994–1998) as an Engineer with Jahad Daneshgahi Elm Va Sanat (JDEVS). Since 1998, he has been an Assistant Professor with the Iran University of Science and Technology. His research interests include power electronics, medium voltage converter topologies, and electrical machines.

MOKHTAR BOZORG (Member, IEEE) received the B.Sc. and M.Sc. degrees in electrical engineering from the Sharif University of Technology, Tehran, Iran, in 2008 and 2011, respectively and the Ph.D. degree, in 2015. In 2011, he joined the Power System Research Group, Ecole Polytechnique Fédérale de Lausanne (EPFL), Lausanne, Switzerland. From 2015 to 2018, he was a Postdoctoral Fellow and a Guest Scientist with the Distributed Electrical System Laboratory, EPFL. Since 2019, he has been an Associate Professor in energy and power systems with the School of Management and Engineering (HEIG-VD), Institute of Energy and Electrical Systems (IESE), University of Applied Sciences Western Switzerland (HES-SO). His research interests include smart grids and active distribution networks, applications of mathematical modeling, optimization techniques, data analytics in power systems, integration of renewable energy sources, and energy storage systems into power systems.

HAMED JAFARI KALEYBAR (Member, IEEE) received the M.S. degree in electrical engineering from the Iran University of Science and Technology, in 2013, and the joint Ph.D. degree from the Sahand University of Technology and Politecncio di Milano, in 2019. From 2019 to 2022, he was a Postdoctoral Research Fellow with the Energy Department, Politecnico di Milano. He is currently an Assistant Professor with the Department of Energy, Politecnico di Milano. His research interests include electric transportation systems, electric railway, power quality control techniques, smart grids, renewable energy sources, and power electronics converters. He is a member of the CIFI (Italian Group of Engineering about Railways).

Open Access funding provided by 'Politecnico di Milano' within the CRUI CARE Agreement